Smart Structures and Systems, *Vol. 28, No. 5 (2021) 643-660*
https://doi.org/10.12989/sss.2021.28.5.643

Structural damage identification for elements and connections using an improved genetic algorithm

Meysam Ramezani [a] and Omid Bahar*

International Institute of Earthquake Engineering and Seismology (IIEES), P.O. Box 1953714453, Tehran, Iran

(*Received April 16, 2020, Revised May 8, 2021, Accepted August 15, 2021*)

Abstract. All structures are exposed to damage during their lifetime. Timely detection of the damages can prevent the reduction of stiffness/resistance of structures. The large number of elements in structures in comparison to the number of measurable data can limit the performance of the closed-form methods. This study presents a new damage detection method determining damage severity and location in the elements and connections via Improved Genetic Algorithm (IGA) based on limited number of mode shapes. This study describes how damage can be accurately identified based on the least number of modes. In this approach, healthy elements are identified by the IGA algorithm and removed from the search space. In this way, the damaged elements are examined more carefully and the severity of the damage is estimated more accurately. In this study, to evaluate the performance of the proposed method, two numerical examples are used. The numerical study includes a 2D truss structure under 4 damage scenarios and a 3D structure with a much larger number of elements under 6 different damage scenarios. Moreover, the performance of this algorithm in presence of noise in modal information is also examined. The results show that the proposed method can accurately detect damage to elements and connections, even in the presence of noise, by using only one mode in the 2D truss and two modes in the 3D structure. In order to evaluate the efficiency of this method in determining the damage of connections, a cantilever beam has been modeled and experimentally tested. The connection stiffness of the beam has been computed using both IGA and load-deformation measurement methods. In the IGA method only the first mode shape of the beam is employed to determine the connection stiffness. To derive the mode shapes in rotational degrees of freedoms which contain valuable information on connection stiffness, a novel, straightforward, and practical approach has been proposed. The results also indicate the high performance of this method to accurately estimate the connection stiffness.

Keywords: 3D structure; element damage detection; experimental connection damage detection; improved genetic algorithm; modal strain energy; model updating

1. Introduction

All civil engineering structures are exposed to damages and deterioration over time due to various hazards and environmental effects. When it passes unnoticed, the spread of the damages can lead to the loss of the overall structural stability. Structural damages reduce stiffness in one or more elements or change their boundary conditions. Vibration characteristics of a structure (i.e., natural frequencies and mode shapes) depend on its dynamic properties (i.e., mass and stiffness) and make it possible to develop methods for detecting structural damage and health monitoring process. However, the primary suggested methods were not successful since there were some noises in the measurements being less sensitive to the damages of the whole structure (Doebling *et al*. 1998). The performance of these methods was acceptable when very precise measurement tools were used for the reduction of noise-signal ratio, or the severity of the structural damage was significant (Whalen 2008).

Due to the limited success of previous methods, several studies focused on employing new approaches such as mode shape curvature, modal strain energy, methods based on flexibility matrix, and the others containing more accurate information about the damage location (Alvandi and Cremona 2006, Pandey and Biswas 1994, Quaranta *et al*. 2016, Shi *et al*. 1998).

The flexibility matrix is more sensitive to changes in low-frequency modes. However, to form a flexibility matrix based on dynamic relationships, several structural modes will be required. In addition, the flexibility matrix obtained from this method is less accurate than direct methods.

Pandey and Biswas (1994) studied the detection of the damaged elements with a limited number of low-frequency modes. Yang and Liu (2009) suggested an algorithm that enabled both qualitative and quantitative detection of the damaged elements based on flexibility changes. Li *et al*. (2010) were able to reduce the effect of removing higher modes in the damage identification process by defining a generalized flexibility matrix instead of the conventional flexibility matrix. Meng *et al*. (2019) applied the modal flexibility method in order to identify the damage in a suspension bridge. Their methods required modal parameters of the bridge that could be achieved through ambient vibration. They compared this method with other

*Corresponding author, Associate Professor,
E-mail: Omidbahar@iiees.ac.ir
[a] Ph.D. Candidate, E-mail: Ramezani.meysam@ut.ac.ir

ISSN: 1738-1584 (Print), 1738-1991 (Online)

classical techniques.

Modal Strain Energy (MSE) is another parameter considered for damage detection. This parameter is obtained from the stiffness matrix and mode shapes of the structure. MSE is very sensitive to structural damages. For example, Shi *et al*. (2000) developed a method based on MSE changes of each element before and after damage. In this method, the elements with remarkable MSE changes were assumed as potential damaged elements. In this regard, a quantitative step is taken for determining the damage location and severity using sensitivity analysis. These methods require a Finite-Element Model (FEM) to calculate the sensitivity of MSE in damaged elements. This method was further improved by Moradipour *et al*. (2015) via reducing numerical errors. Moreover, some researchers (Yan *et al*. 2010, Yan and Ren 2014) determined the damaged elements using a closed-form of MSE sensitivity and generalized flexibility sensitivity. The advantage of this method was its efficiency in one step without trial and error, and providing appropriate results in the case of eliminating higher modes.

Shahri and Ghorbani-Tanha (2017) provided a method based on modal kinetic energy change for damage detection. The advantage of this method over other MSE methods was its lower sensitivity to the noises in mode shapes and achieving acceptable results while dealing with noises in frequency. Liang *et al*. (2019) proposed combining the cross-model and cross-mode for updating FEM based on the frequency-change-ratio. They experimentally verified this method to locate damages in several shear buildings.

Instead of using mod shapes to obtain spatial information, the derivatives of mode shapes such as mode curvature can be alternatively used. The positive effect of rotational Degrees Of Freedom (DOFs) on structural health monitoring and damage identification problems has been proven. Due to the difficulties of extracting rotational response, some researchers have tried to indirectly extract the effect of this response through translational responses. Datta and Dutta (2020) investigated the effect of rotational DOFs in improving the estimation of the stiffness matrix for the ASCE standard structure. By assigning mass to rotational DOFs and using an iterative technique, they estimated the structural mode shapes including the translational and rotational DOFs and showed that the proposed method provides a more accurate estimate of the stiffness matrix compared to the method with only translational DOFs. Due to the numerical errors in this method and consequently the reduced performance in real examples, the researchers used rotation sensors to directly measure the response of rotational DOFs. Although the positive effect of using rotational response to understand structural behavior has been proven, limited studies have been performed on direct measurement of rotation to identify damage (Alten *et al*. 2017, Hester *et al*. 2020, Huseynov *et al*. 2020, Ramezani and Bahar 2021). Huseynov *et al*. (2020) evaluated a simply supported beam both numerically and experimentally using direct rotation measurements. In their study, sensitivity of rotation to damage and the effect of sensor locations on sensor sensitivities were studied. They showed that the use of modal information alone to detect damage was not satisfactory, and that the use of strain gauge sensors could detect some damage only when the strain gauges were installed near the damage location. Conversely, rotation measurements led to satisfactory results for all scenarios.

From the mathematical point of view, damage detection includes many non-linear equations. Hence, heuristic algorithms can be used to detect the damages in structures (Ding *et al*. 2019, Gomes *et al*. 2019, Kaveh *et al*. 2019, Zheng *et al*. 2020, Hormozabad and Soto 2021). In this regard, Gomes and Silva (2008) identified damaged elements using frequency sensitivity method and the optimization-based method using Genetic Algorithm (GA) and compared the results. They used the structure frequencies as an input of GA in order to find the damaged elements. Srinivas *et al*. (2011) used a multi-stage damage detection based on the modal strain energy. At first, they used the MSE change ratio for reducing the number of unknown variables. After the reduction of variables, they used GA for the exact detection of damaged elements. Their method was suitable for simple models. For this reason, it was necessary to reduce the variables through the first step.

To detect the damaged elements, Nobahari and Seyedpoor (2011) applied a modified GA by introducing the correlation-based target function. They used the natural frequency changes as the damage criterion. Applying their proposed method, determination of the damage severity requires less analysis compared to the basic GA. Silva *et al*. (2016) applied an unsupervised clustering method to detect the damage in a real bridge and used GA to perform the clustering task.

Pal *et al*. (2017) used vibration-based structural health monitoring techniques to determine the reduction in connection stiffness based on the strain time history. They used the particle swarm optimization algorithm to minimize the objective function. Daei *et al*. (2017) provided an intelligent method for identifying the location and severity of damage based on model optimization. In their method, they used the pseudo-residual forces theory to predict the location and severity of damage to the structure. Their method could identify damage with a limited number of mode shapers. Tiachacht *et al*. (2018) introduced the Modified Cornwell Indicator which performed better on damage detection than the standard form. They used this index for the objective function of the genetic algorithm to be able to quantitatively identify the damage in structural elements. They evaluated the method using several numerical examples of truss structures.

The existences of uncertainties in the FEM parameters and modeling errors are inevitable. In this regard, Ghiasia and Ghasemi (2018) reduced the computational cost of the model updating during the optimization process for damage detection by the use of a trained surrogate model. In their method, the probability density function of undamaged and damaged systems was adopted for calculating the probability of damage existence. Seyedpoor *et al*. (2018) proposed a multi-stage Differential Evolution (DE) algorithm to detect multiple damages in structural systems. They used some natural frequency changes to identify damages in a cantilever beam. Pedram *et al*. (2018)

presented a model updating method based on spectral density function in frequency space. They used some lower and incomplete modes to achieve damage identification. They evaluated their method for several different damage patterns.

Using the enhanced vibrating particles system algorithm, Kaveh *et al*. (2019) identified damage to truss structures with limited available modal information.

Several studies were performed to detect damaged elements and determine the severity of damages. The advantage of each of these studies is their accuracy in detecting the location or severity of damages, despite eliminating higher modes. Furthermore, many of the methods presented so far can only be used for simple and 2D structural systems.

In this study, a novel methodology is presented to extract rotational modes that contain valuable information about damage and stiffness of connections through a simple procedure. If rotational mode shapes are extracted, fewer mods are required for damage identification problems. This goal becomes a reality only when sophisticated tools and ideas are incorporated in the damage identification system. In this study, an Improved Genetic Algorithm (IGA) is proposed to identification damages. This algorithm has been upgraded based on the knowledge of structural dynamics and damage detection. This upgrade makes it possible to investigate 3D structures with a large number of variables and the lowest modal information. This upgrade makes it possible to detect damage in elements and connections based on the information of only one mode in 2D problems and two perpendicular modes in 3D structures. In this study, two numerical examples including a 2D truss and a 3D structure are used to evaluate the proposed method. The performance of this method in the presence of noise will also be examined. A cantilever beam welded to an angle section is constructed to evaluate the performance of the proposed algorithm in detecting connection damage. In this example, the fixity factor of the connection is determined using only the first mode shape.

2. The theoretical background

For an undamped structure with linear behavior, modal characteristics are obtained from the system characteristic equation, as follows

$$\boldsymbol{K}\boldsymbol{\Phi}_i = \lambda_i \boldsymbol{M}\boldsymbol{\Phi}_i \tag{1}$$

where, K and M are respectively $N_D \times N_D$ stiffness and mass matrices of a system with N_D DOFs; λ_i and $\boldsymbol{\Phi}_i$ are frequency and mode shape of i^{th} mode. According to the dependency of dynamic characteristics of the system (natural frequencies and modal shapes) to its physical characteristics (mass and stiffness), when damage occurs in the structure due to different reasons, including earthquake or windstorm, fatigue caused by severe changes in loading or old age, etc., the dynamic characteristics of the system will change under the influence of the damage. On the other hand, the structural damages mostly reduce the stiffness in one or several elements of the system. Using this important point, the convergence speed and performance of the GA will be improved. These damages rarely decrease the mass. Therefore, in this study, the changes in mass matrix are not considered. Hence, the system characteristic equation in damaged condition is expressed as follow

$$\boldsymbol{K}^d\boldsymbol{\Phi}_i^d = \lambda_i^d \boldsymbol{M}\boldsymbol{\Phi}_i^d \tag{2}$$

where, the superscript d indicates the damaged system. The overall stiffness matrix of the system is obtained by assembling stiffness matrices of all structure elements

$$\boldsymbol{K} = \sum_{j=1}^{N_E} \boldsymbol{K}_j \tag{3}$$

in which $\boldsymbol{K}_j$ demonstrates the $N_D \times N_D$ stiffness matrix of the j^{th} element and N_E is the total number of elements. Therefore, the effect of damage to each element on the total stiffness matrix can be expressed as

$$\boldsymbol{K}^d = \boldsymbol{K} + \sum_{j=1}^{N_E} \Delta\boldsymbol{K}_j = \boldsymbol{K} + \sum_{j=1}^{N_E} \alpha_j \boldsymbol{K}_j \tag{4}$$

where, $\Delta\boldsymbol{K}_j$ is the stiffness difference between healthy and damaged elements. The parameter α_j is the stiffness reduction coefficient of elements. Since the stiffness of the damaged elements is less than healthy elements, then $-1 < \alpha_j \leq 0$. In this study, stiffness reduction of elements is defined by assuming the reduction of elasticity modulus of elements and after analysis of the suggested algorithm. This assumption is investigated to determine the type and severity of damage.

2.1 Modal Strain Energy (*MSE*)

MSE, which is obtained from the stiffness matrix of structural elements and second-order mode shape of the system, is very sensitive to the structural damages. MSE of i^{th} mode for j^{th} element before and after the damage is defined according to the following equations

$$MSE_{ij} = \frac{1}{2}\boldsymbol{\Phi}_i{}^T \boldsymbol{K}_j \boldsymbol{\Phi}_i \tag{5}$$

$$MSE_{ij}^d = \frac{1}{2}\boldsymbol{\Phi}_i^{dT} \boldsymbol{K}_j^d \boldsymbol{\Phi}_i^d \tag{6}$$

Because the damaged elements are unknown, the stiffness matrices estimated by IGA in every step are used to calculate MSE in the damaged case (Shi *et al*. 1998)

$$MSE_{ij}^d = \frac{1}{2}\boldsymbol{\Phi}_i^{dT} \boldsymbol{K}_j^{pd} \boldsymbol{\Phi}_i^d \tag{7}$$

where, the superscript pd indicates the probability of damage.

3. Genetic algorithm

Biological processes happening in living nature, such as reproduction, mating, and mutation, are the basis of a heuristic algorithm, called genetic algorithm. The GA is a potent search and optimization technique that reviews the problem space randomly and step by step. On average, GA gives better responses in each step compared to the previous step and continues until achieving the desired convergence regarding the accuracy of a problem (Ramezani *et al*. 2017).

In this study, by applying several changes to the standard process of the genetic algorithm, this algorithm becomes a powerful and efficient tool for solving damage detection problems**.** Also, with a proper definition of fitness functions and the desired constraints in damage detection, this algorithm tries to find the appropriate responses using trial and error and maintain the good patterns after evaluation. Repeating this process, the best response is obtained which satisfies all the constraints and minimizes the fitness function.

3.1 Damage detection of structural elements using IGA

In this study, IGA is used to determine the damage severity and location in damaged elements of the structure. Since structural damage detection methods aim to find the element stiffness reduction coefficient (α_j), this parameter is introduced as an output from the IGA. Continuing the analysis process, the reduction of fitness function to catch zero indicates the coincidence of the analysis model between the updated structure and the damaged structure. In the case of convergence and observing non-zero value for fitness function, which means a possibility of unknown damage occurrence in structure, the finding is not included in the algorithm. In this study, the possibility of damage occurrence caused by the change of the boundary conditions of element connections is investigated in the final step. The damage severity of elements is determined by the IGA according to the following levels:

1) First, by specifying the change limit of output parameters ($-1 < \alpha_j \leq 0$), a set of chromosomes which are randomly assigned either 0 or 1 is created. Each chromosome contains information about the stiffness reduction coefficient of structure elements. Then, different parts of the produced chromosomes are transferred to basis 10, to produce a set of real numbers that are the stiffness reduction coefficient of structure elements. In the next level, the finite element model is created in which its geometric characteristics are entirely identical to the primary structure model, and the produced damage coefficients are assigned to its elements employing IGA. Regarding the following equation, MSE of the j^{th} element in i^{th} mode is calculated

$$MSE_{ij}^{pd} = \frac{1}{2}\boldsymbol{\Phi}_i^{pd^T}\boldsymbol{K}_j^{pd}\boldsymbol{\Phi}_i^{pd} \tag{8}$$

Since the ASCE benchmark problem is a 3D structure and the stiffness of some elements, such as braces, is zero in perpendicular directions, if a translational mode is used, the product of the translational mode shape and the stiffness of the brace elements will be zero. This can happen due to the presence of zero components in the mode shape, at DOFs defining the stiffness of the brace. In this case, with any change in the stiffness of the brace, the strain energy will always be zero, and as a result, if there is damage to these elements, it will not be reflected in strain energy. Thus, by using the total strain energy of two perpendicular modes in the structure, it can be ensured that the properties of the updated model converge to the properties of the damaged structure. But in 2D models, the MSE of elements have nonzero values in all modes, and the MSE value also changes due to the changes in stiffness of the elements. For this reason, in 2D models, the damage can be identified by having only one mode**.** Due to the fact that the lower modes of structures are usually the simplest modes to measure, the first mode of the 2D structure and the first two modes of the ASCE 3D structure (in two longitudinal and transverse directions perpendicular to each other) are used to calculate the strain energy changes.

By calculating the MSE of elements using parameters estimated by IGA, MSE changes of j^{th} element in i^{th} modes, are calculated according to the following equation

$$\Delta\text{MSE}_{ij} = MSE_{ij}^{d} - MSE_{ij}^{pd} \tag{9}$$

In order to increase the convergence speed, the MSE variation and the difference between the frequencies of the damaged structure and the frequencies estimated by the algorithm are used to define the objective function.

$$OF = \sqrt{\sum_{j=1}^{NE}\left(\left(\sum_{i=1}^{NM}\left|\Delta\text{MSE}_{ij}\right|\right)^2\right) + \sum_{i}\Delta f^2} \tag{10}$$

Where OF represents the objective function, Δf is the difference between frequencies in the damaged structure and the analytical model estimated by the algorithm, and NM is the number of modes used to calculateΔMSE, which is equal to 1 in the 2D model and equal to 2 in the 3D model with perpendicular braces.

It is worth noting that if the stiffness reduction coefficient of elements is estimated correctly with IGA, the MSE changes will be zero. Hence, damage assumption of elements is correct due to their elasticity modulus reduction. It implies that damage occurs in the element's length. Otherwise, assuming the change in stiffness matrix coefficient, i.e., elasticity modulus, is not entirely responsible for changes, and it is necessary to check element connection conditions in the ends of the element. In other words, the possibility of damage in element connections susceptible to damage should be accurately evaluated. Accordingly, the target of IGA is minimizing the sum of MSE changes of all elements in any desired (available) mode.

2) In the next step, chromosomes are classified based on the smallest MSE changes being the most fitness to the

objective function. The most adaptive chromosome to the damaged structure is the one that creates the lowest fitness function. In the following, the chromosomes with most adaptations are used for reproduction to create the children chromosomes. In order to avoid stopping the IGA process in probable local minimization, the mutation operator changes the binary numbers of chromosomes with a 2% possibility. Then, the new chromosomes are used to determine the fitness. In this study, the concept of "elitism" is used at every level of new chromosome creation. Regarding this concept, the best chromosome of each generation is transmitted into the next generation without any changes. This process leads to maintain the suitable genes of the chromosome, and facilitates the convergence process. This cycle continues until the fitness function becomes less than the amount determined by the user, or any improvement in results is achieved during specific repetitions.

3) Up to this point, the basis of the standard GA algorithm was described. By applying the following steps to the standard algorithm, it can be turned into a powerful tool for accurate damage detection with rapid convergence.

3-1) Damages usually occur in limited number of elements; therefore, as a solution for the rapid identification, the damage coefficients of one of the chromosomes in the first generation is assumed zero. This assumption helps to improve the value of the objective function at the beginning of the process compared to randomly selected values (yellow color in Fig. 1)

3-2) The majority of damage identification algorithms proposed by other researchers work well in simple structures with limited elements. But as the number of structural elements increases and as a result the number of algorithm variables increases, those methods face challenges. In the proposed algorithm however, using a novel approach for damage detection in elements, after the convergence of the algorithm, elements whose damage coefficients are estimated to be less than 1%, are identified as healthy elements and removed from the search space. This threshold for separating healthy and damaged elements can be increased depending on the accuracy of the method and the noise in the data. In fact, this threshold can be called the reliability level of the results. This process leads to a reduction in the number of variables thereby providing a more accurate search to identify damaged elements (orange color in Fig. 1).

3-3) After each convergence and removal of healthy elements from the search space, the algorithm needs to resume searching with a smaller number of elements. One of the best responses that can enter the first population at the beginning of the process is the best response from the previous repetition, because this response has valuable

Table 1 The IGA parameters

The population of generations	10
Max. number of generations	100 for Ex1, 400 for Ex2, 200 for Ex3
The number of variables	47 for Ex1, 116 for Ex2, 2 for Ex3
The range of variables	$[-1,0]$ for elements, 0 and 1 for connections
Objective function	Eq. (10)
Mutation rate	0.02
Coding	Binary
Selection	Roulette wheel
Crossover	Uniform crossover binary

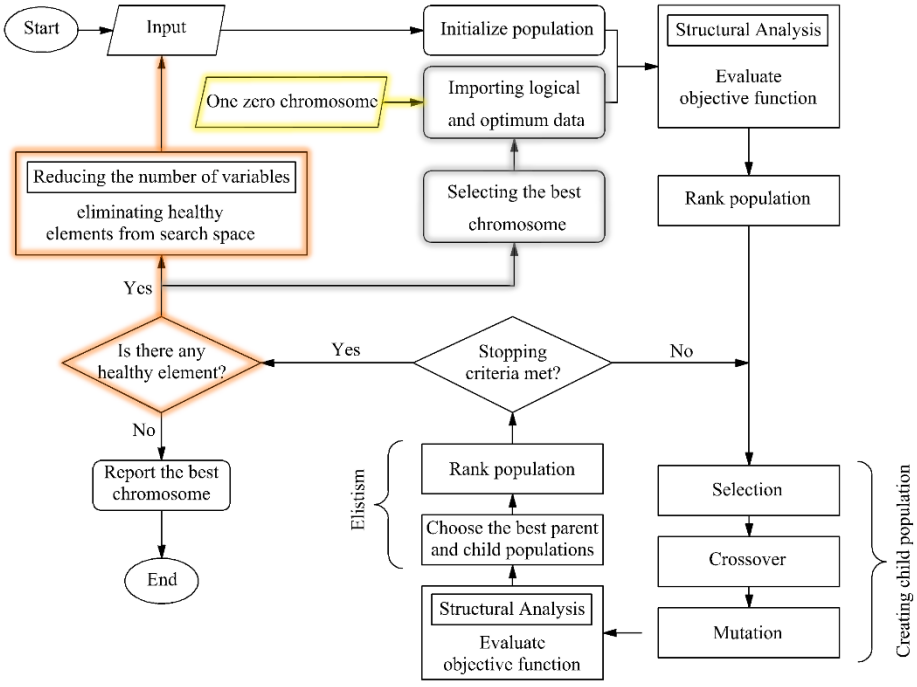

Fig. 1 Steps to determine the severity of damage in structural elements using IGA

genes and can attract other elements of the population and produce children with higher fitness values (purple color in Fig. 1)

This process continues until no healthy element is identified among the elements after temporary convergence. At this stage, the best answer is reported as the final solution**.** The characteristics and parameter values of the IGA are presented in Table 1.

4. Numerical simulations

Two different examples have been used to evaluate the performance of the proposed method. In the process of data acquisition of the damaged structures, complete noise removal is impossible. The presence of noise in the data measured by sensors causes a deviation from exact modal information. In order to simulate the effect of noise, the mode shapes and frequencies are contaminated with different noise levels (0%, 1%, 3% and 5%). The noise-contaminated mode shapes are obtained through the following equation.

$$\bar{\Phi}_{ir} = \Phi_{ir}(1 + \gamma_r^{\Phi}\rho^{\Phi}\left|\Phi_{max,i}\right|) \quad (11)$$

$$\bar{\omega}_i = \omega_i(1 + \gamma^{\omega}\rho^{\omega}) \quad (12)$$

Where $\bar{\Phi}_{ir}$ and Φ_{ir} are the r^{th} components of the i^{th} mode with and without noise, respectively. γ_r^{Φ} and γ^{ω} are the Gaussian random numbers with zero mean and variance equal to one; ρ^{Φ} and ρ^{ω} are the noise level imposed on the mode shapes and natural frequencies; and $\left|\Phi_{max,i}\right|$ is the largest absolute value among mode shape components without noise; $\bar{\omega}_i$ and ω_i are the i^{th} natural frequency with and without noise, respectively. Since the generated random numbers can affect the estimated damage severities, the damage severities are estimated based on 10 different random numbers and the average results are reported in the tables.

4.1 2D truss

In the second example, a planar steel truss (Seyedpoor *et al*. 2018) containing 47 bars, 22 nodes and 41 DOFs is considered as shown in Fig. 2.

The simulated planar truss is considered as a steel truss where $E = 30000$ ksi , $\rho = 0.3$ lb/in^3 and the cross-sectionional area of the bars are assumed 2 in^2. As shown in Table 2, four different damage scenarios and damage severities are used for examination of the proposed method.

4.1.1 Investigating the proposed damage detection method in the 2D truss

The convergence processes of the objective function of planar truss are shown in Fig. 3. This figure contains two types of curves: “maximum population fitness” and “mean population fitness.” The “maximum population fitness” curve indicates the performance of the best chromosome in each generation. This line remains horizontal in some generations where the children chromosomes do not show

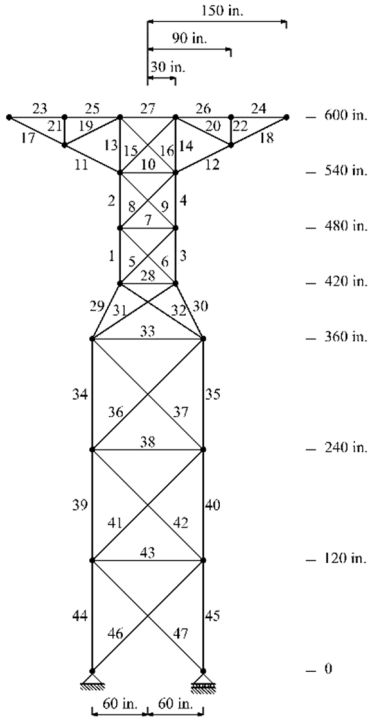

Fig. 2 Configuration of the 47-bar truss structure

Table 2 Damage Scenarios of the 47-bar truss

Damage scenario	Damaged element(s)	Damage severity
DS1 Single damage	No. 10	30%
DS2 Single damage	No. 30	30%
DS3 Double damage	No. 10, No. 30	30%, 30%
DS4 Double damage	No. 40, No. 41	30%, 20%

fitness values higher than the parent chromosomes. In this case, the best chromosome of each generation is passed directly to the next generation due to elitism. This will prevent the algorithm from deviating from the optimal state sue to the production of inappropriate children. The “mean population fitness” curve indicates the compatibility average of each generation according to the objective function. The presence of an elite chromosome in each generation leads to its integration with other chromosomes which results in the production of a new generation that are very similar to the parent chromosomes. Therefore, this graph is always descending.

In the IGA convergence process, the number inside the circles shows the number of the residual variables (elements) in each iteration. According to this figure, in all scenarios, 47 truss elements were first introduced to the algorithm, and after resuming the search process and removing the healthy elements for the next iterations, the damaged elements were accurately identified. In Fig. 4, the severity of the damage obtained from the proposed algorithm is presented. The difference between this value and the severity of the damage to the model under different noise percentages is shown in Table 3.

ΔDS is obtained through the following equation.

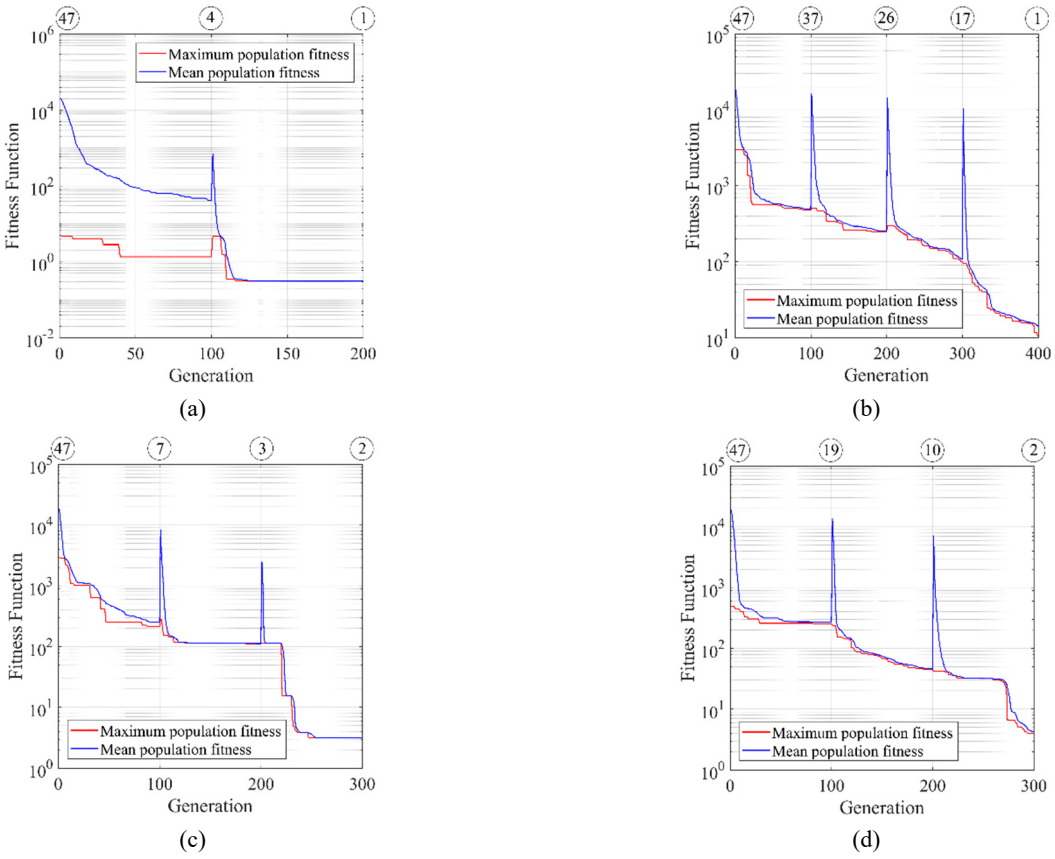

Fig. 3 The convergence process of the Fitness function obtained by IGA (a) DS1; (b) DS2; (c) DS3; (d) DS4 (0% noise level)

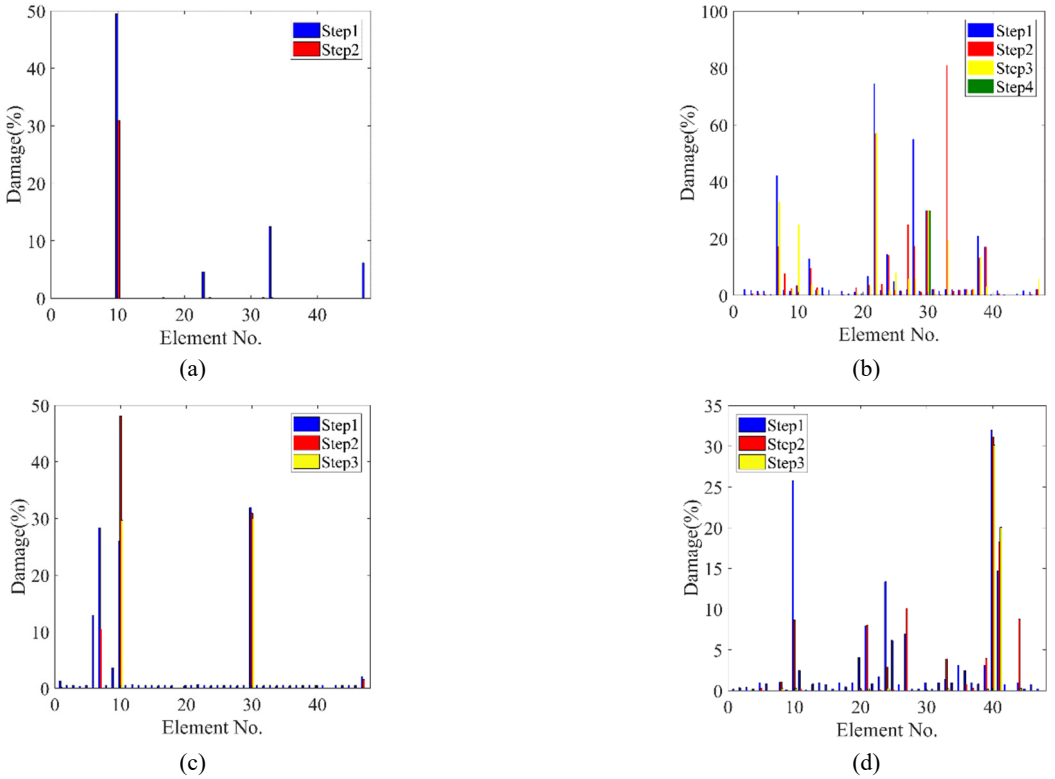

Fig. 4 Damage severity of the 2D truss estimated by IGA in (a) DS1; (b) DS2; (c) DS3; (d) DS4 (0% noise level)

Table 3 Damage severity in elements

DS	No. element	Damage severity				ΔDS (%)			
		NoiselLevel				Noise level			
		0%	1%	3%	5%	0%	1%	3%	5%
DS1	10	30.01	30.37	31.61	32.27	1.17×10^{-2}	3.72×10^{-1}	1.61×10^{0}	2.27×10^{0}
	Average					1.17×10^{-2}	3.72×10^{-1}	1.61×10^{0}	2.27×10^{0}
DS2	30	30.00	30.03	30.03	29.63	3.11×10^{-3}	2.73×10^{-2}	2.92×10^{-2}	3.75×10^{-1}
	Average					3.11×10^{-3}	2.73×10^{-2}	2.92×10^{-2}	3.75×10^{-1}
DS3	10	30.01	29.77	30.14	30.25	5.29×10^{-3}	2.31×10^{-1}	1.40×10^{-1}	2.49×10^{-1}
	30	29.99	29.98	30.15	30.31	8.86×10^{-3}	2.14×10^{-2}	1.47×10^{-1}	3.17×10^{-1}
	Average					7.08×10^{-3}	1.26×10^{-1}	1.44×10^{-1}	2.83×10^{-1}
DS4	40	30.03	30.04	29.97	29.87	2.99×10^{-2}	3.97×10^{-2}	2.86×10^{-2}	1.29×10^{-1}
	41	20.08	19.94	20.21	20.54	7.59×10^{-2}	5.88×10^{-2}	2.11×10^{-1}	5.45×10^{-1}
	Average					5.29×10^{-2}	4.92×10^{-2}	1.20×10^{-1}	3.37×10^{-1}

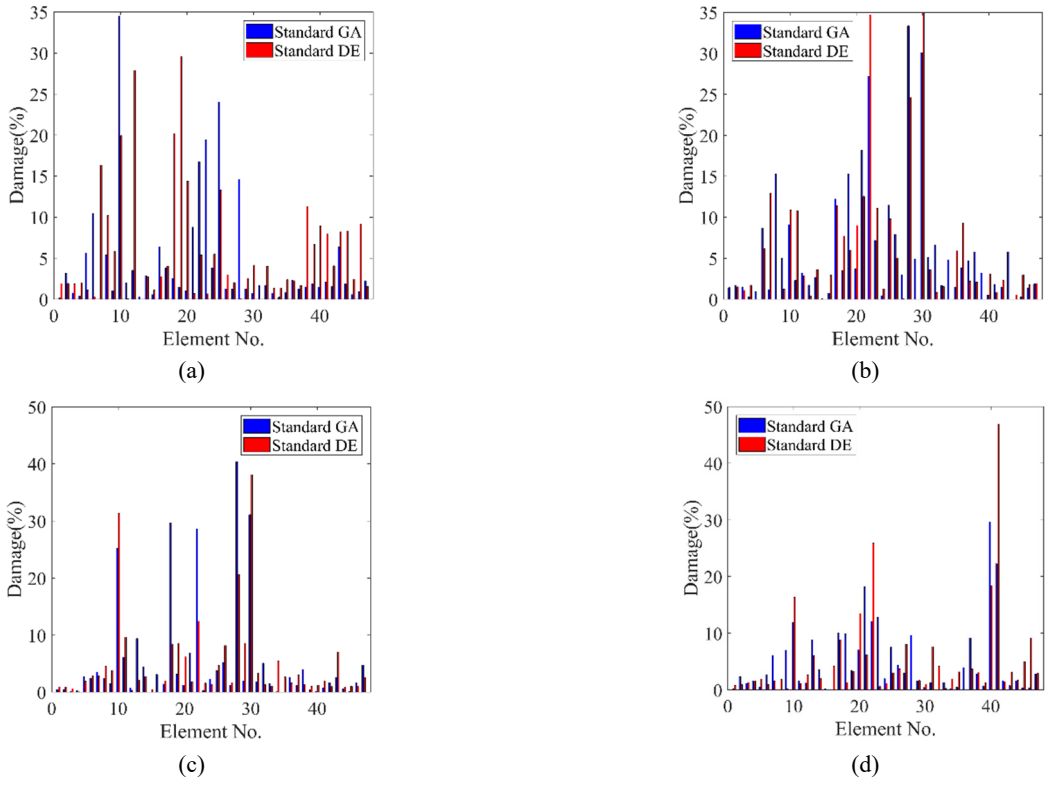

Fig. 5 Damage severity of the 2D truss estimated by the standard GA and DE in (a) DS1, (b) DS2 (0% noise level)

$$\Delta DS = |DS_{\text{Estimated}} - DS_{\text{Exact}}| \quad (13)$$

where ΔDS is the difference in damage severity, $DS_{\text{Estimated}}$ is the damage severity estimated by the proposed algorithm, and DS_{Exact}represents the exact damage severity. In order to clarify the effect of using the IGA algorithm on the accuracy of the results presented in Table 3, this problem is also solved by the standard GA considering 0% noise. In Fig. 5, damage severities estimated by the standard GA and DE algorithms after 1000 generations are presented. Only one mode, third mode, is used to identify the damages of this model by the proposed algorithm, while the first three modes of this structure are used to identify the damages by the standard GA and DE algorithms. As can be seen, the IGA algorithm estimates the severity of the damage much more accurately and with fewer generations. The reason for this difference is the ideas implemented in the IGA algorithm.

4.2 3D ASCE benchmark

In the second example, the ASCE benchmark structure is evaluated (Johnson *et al*. 2004). This structure includes four floors and two bays in both directions with 1.25 m

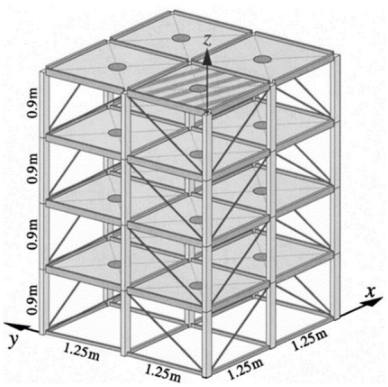

Fig. 6 Analytical model of ASCE benchmark structure (Johnson *et al*. 2004)

Table 4 Numbering of different groups of elements

Story	Elements number of different groups		
	Columns	Beams	Braces
1	$[1-9]$	$[10-21]$	$[22-29]$
2	$[30-38]$	$[39-50]$	$[51-58]$
3	$[59-67]$	$[68-79]$	$[80-87]$
4	$[88-96]$	$[97-108]$	$[109-116]$

dimension. The height of every floor is 0.9 m, and the total height is 3.6 m. The analytical model of the structure is shown in Fig. 6. This structure contains 36 columns, 48 beams, and 32 bracing elements. The columns, beams, and braces of the different floors are numbered according to Table 4. The beam-column connections of this structure are assumed rigid. Element sections are designed for a scaled model, and their characteristics are presented in Table 5.

In this study, a 120-DOF model of the structure is used for damage detection. In this state, the horizontal transition and in-plain rotation for available nodes of each alignment are considered equal. The slab of each floor is assumed to have only in-plane stiffness that makes the slab act rigidly.

The damages of the benchmark structure can be simulated by eliminating some elements or replacing them with weaker elements. Six different damage scenarios are defined for this structure as follows:

- Scenario 1: all braces of the first floor are destroyed (i.e., these braces contribute mass, but provide no resistance within the structure)
- Scenario 2: all braces of the first and third floors are destroyed.
- Scenario 3: one of the braces of the first floor is destroyed.
- Scenario 4: one of the braces of the first and third floors are destroyed.
- Scenario 5: the stiffness of one of the braces of the first floor is reduced to 2/3 of its initial value.
- Scenario 6: in addition to damages of scenario 4, the end of one of the first-floor beams is also destroyed, and it only transmits forces and cannot sustain any bending moments. Table 6 presents the natural frequencies of healthy and damaged structure. For damage detection, the first two modes of structure in x and y direction are used.

4.2.1 Investigating the proposed damage detection method in the 3D ASCE model

According to the proposed method, in order to determine the stiffness reduction coefficient of each element, a corresponding variable should be defined in IGA. Considering the existence of 116 elements in the structure, defining all these variables simultaneously in this algorithm can reduce its performance. Therefore, damage detection is performed separately in different groups of elements, including braces, columns, and beams.

Since braces are more vulnerable elements in braced steel structures, and the damage is more likely to first happen in brace elements, it is helpful to examine this group first. In this way, if the objective function converges to zero, the other groups do not need to be examined. However, in this study, in order to perform the complete search process, all groups regardless of the objective function results are examined. According to the explanations described in

Table 6 Natural frequencies of analytical models (Hz)

Mode No.	1	2	3	4
Undamaged	8.588	9.181	14.580	23.452
Scenario 1	5.468	7.373	9.691	19.315
Scenario 2	4.965	6.685	8.703	12.340
Scenario 3	8.093	9.181	14.204	22.474
Scenario 4	8.092	8.953	14.041	22.450
Scenario 5	8.455	9.181	14.471	23.149
Scenario 6	8.042	8.953	14.041	22.423

Table 5 Characteristics of ASCE benchmark structure sections

Properties	Columns	Beams	Braces
Section type	$\mathrm{B100\times 9}$	$\mathrm{S75\times 11}$	$\mathrm{L25\times 25\times 3}$
Cross-sectional area $A(m^2)$	1.13×10^{-3}	1.43×10^{-3}	1.41×10^{-4}
Moment of inertia (strong direction) $I_y(m^4)$	1.97×10^{-6}	1.22×10^{-6}	0
Moment of inertia (weak direction) $I_z(m^4)$	6.64×10^{-7}	2.49×10^{-7}	0
St. Venant torsion constant $J(m^4)$	8.01×10^{-9}	3.82×10^{-8}	0
Young's modulus$E$(Pa)	2×10^{11}	2×10^{11}	2×10^{11}
Mass per unit volume (kg/m^3)	7800	7800	7800

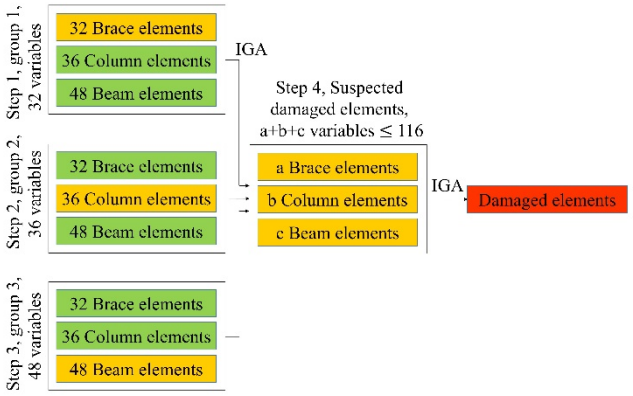

Fig. 7 Classifying elements in different groups, and identifying damage

the first step, 32 brace elements are examined as the first group.

Assigning the damage coefficients for input elements (i.e., braces) and assuming the other structure elements as healthy (i.e., columns and beams), the algorithm detects the damage in brace elements. This step is only done with the aim of separating undamaged elements from damaged ones. The second and third steps are done for beam and column groups similar to the first step. Up to the end of the third step, the results demonstrate a limited set of elements suspicious for damage including several braces, beams, and columns. In the fourth step, all the elements diagnosed as damaged, at the end of the first to third steps, are studied together. These steps are shown in Fig. 7. In Fig. 7 and Table 7, green, yellow, and red colors represent healthy, suspected damaged, and damaged elements, respectively.

In order to facilitate and expedite the damage detection process, the damage coefficients of input elements at the end of the first to third steps, enter the first generation of the fourth step in the IGA search as a worthy chromosome. Search in the fourth step continues until the undamaged elements are eliminated from the search space. Reducing the search space in each repetition, the damage coefficients are determined more precisely. If no undamaged element is detected in one of the repetitions, and the search space is not reduced, this process will be stopped. At the end of the fourth step, the fitness function is checked out. If the fitness function is close enough to zero, it can be concluded that: 1) the locations of damaged elements are detected correctly, and 2) the damage is a type of elasticity modulus reduction. Therefore, the damage coefficients are extracted accurately.

However, if the fitness function converges to a non-zero value, only the results related to suspected damaged elements are reliable. In the following, to determine the type and severity of actual damage, the damage possibility in connections is added to the states, and the problem is investigated again. According to damage Scenario 1, all braces in the first floor are eliminated. As mentioned earlier, in the first step, the elements of the brace group are studied. The process of identifying damaged elements for brace elements group due to damage Scenario 1 and a noise level of 0% is shown in Table 7. As indicated in Table 7, after four repetitions of IGA, 32 potentially damaged brace

Table 7 Damage coefficients of brace elements estimated by IGA for Scenario 1 (0% noise level)

Story	No. elements	Damages (%)			
		Step 1	Step 2	Step 3	Step 4
1	22	99.7	99.9	100	100
	23	99.9	99.8	100	100
	24	99.2	100	100	100
	25	100	100	100	100
	26	99.9	100	100	100
	27	99.6	100	100	100
	28	99.9	100	100	100
	29	99.9	100	100	100
2	51	2.1	0.6	H	H
	52	1.6	0.4	H	H
	53	0.2	H	H	H
	54	0.2	H	H	H
	55	2.1	0.3	H	H
	56	0.0	H	H	H
	57	0.9	H	H	H
	58	0.6	H	H	H
3	80	2.3	0.6	H	H
	81	0.3	H	H	H
	82	2.3	0.4	H	H
	83	0.2	H	H	H
	84	4.0	0.9	H	H
	85	0.4	H	H	H
	86	0.6	H	H	H
	87	0.4	H	H	H
4	109	18.2	0.0	H	H
	110	22.5	0.6	H	H
	111	4.3	2.5	0.1	H
	112	36.4	5.6	0.2	H
	113	3.9	0.1	H	H
	114	5.9	5.2	0.2	H
	115	4.7	3.2	0.1	H
	116	8.5	14.6	0.4	H

elements are narrowed down to 8 elements suspicious to damage. Steps two to four that include columns, beams, and the elements suspicious to damage remaining from the past three groups of suspected damaged components, are performed similar to the first step. The convergence results of fitness function during consecutive generations are shown in Fig. 8. Studying three groups of braces, columns, and beams (Figs. 8(a), (b), (c)), 84 elements enter the fourth step as the elements suspicious to damage (Fig. 8(d)).

The fitness function value in the last search generation of the algorithm for different groups is presented in Table 8. Since the fitness function for the brace group converges to zero, it can be concluded that all damaged elements are in

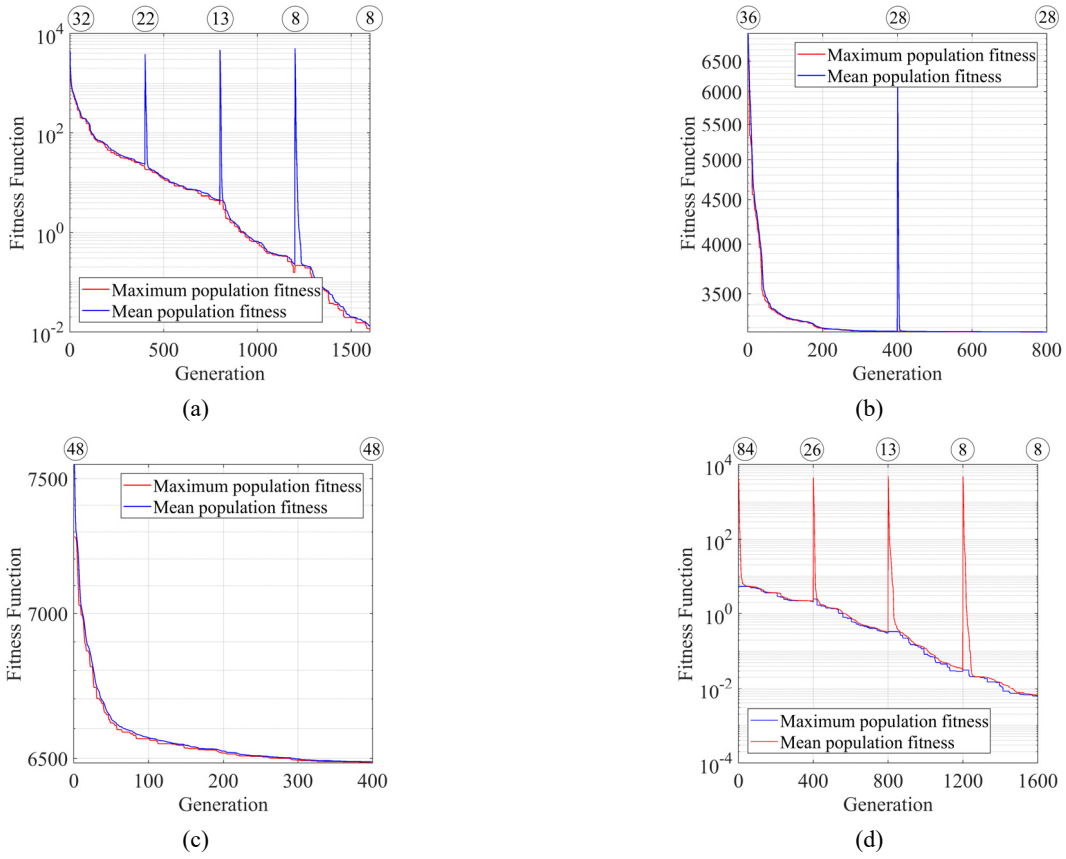

Fig. 8 The convergence process of the fitness function obtained by IGA for Scenario 1. (a) Braces group; (b) Columns group; (c) Beams group; (d) Suspected damaged elements (0% noise level)

Table 8 Final fitness function of different groups estimated by IGA for Scenario 1 (0% noise level)

Steps	Groups	Fitness function
1	Braces	0.0116
2	Columns	3163.8519
3	Beams	6485.2125
4	Suspected damaged elements	0.0066

the brace group. Furthermore, in this group, the damaged elements are well recognized. However, in order to complete the damage detection process, the other groups are studied as well. In this scenario, regarding the convergence of fitness function to zero in the fourth step, it can be concluded that location and severity of damaged elements are recognized accurately, and the damage is in form of elasticity modulus reduction. The values of fitness function obtained from beam and column groups imply that damage

Table 9 Damage severity in elements estimated by IGA for Scenario 1

No. element	Damage severity				ΔDS (%)			
	Noise level				Noise level			
	0%	1%	3%	5%	0%	1%	3%	5%
22	100.00	99.75	99.30	99.50	2.58×10^{-7}	2.53×10^{-1}	7.03×10^{-1}	5.02×10^{-1}
23	100.00	99.95	99.79	99.23	3.29×10^{-9}	5.15×10^{-2}	2.13×10^{-1}	7.74×10^{-1}
24	100.00	99.41	99.87	98.82	1.84×10^{-7}	5.95×10^{-1}	1.34×10^{-1}	1.18×10^{0}
25	100.00	99.90	99.21	99.76	8.62×10^{-9}	9.82×10^{-2}	7.89×10^{-1}	2.34×10^{-1}
26	100.00	99.89	99.76	99.00	4.63×10^{-8}	1.15×10^{-1}	2.23×10^{-1}	1.00×10^{0}
27	100.00	99.86	99.29	99.53	3.83×10^{-6}	1.36×10^{-1}	7.06×10^{-1}	4.66×10^{-1}
28	100.00	99.74	99.25	99.24	1.06×10^{-7}	2.64×10^{-1}	7.45×10^{-1}	7.62×10^{-1}
29	100.00	99.79	99.76	99.55	1.21×10^{-7}	2.14×10^{-1}	2.44×10^{-1}	4.49×10^{-1}
Average					5.70×10^{-7}	2.16×10^{-1}	4.70×10^{-1}	6.71×10^{-1}

exists in elements other than these groups because regardless of efforts to adapt the updated model, satisfactory results are not achieved.

The results of damage detection obtained from the fourth step are presented in Table 9. The results presented in this table show that the proposed algorithm is capable of

Table 10 Damage severity in elements estimated by IGA for Scenario 2

No. element	Damage severity				ΔDS (%)			
	Noise level				Noise level			
	0%	1%	3%	5%	0%	1%	3%	5%
22	100.00	99.78	99.48	99.37	1.11×10^{-3}	2.22×10^{-1}	5.25×10^{-1}	6.33×10^{-1}
23	100.00	99.95	99.73	99.69	9.94×10^{-4}	5.13×10^{-2}	2.67×10^{-1}	1.31×10^{0}
24	100.00	99.79	99.76	99.32	3.05×10^{-4}	2.07×10^{-1}	1.24×10^{0}	6.76×10^{-1}
25	100.00	99.60	99.55	98.94	6.53×10^{-5}	3.95×10^{-1}	4.52×10^{-1}	1.06×10^{0}
26	100.00	99.93	99.50	98.31	4.70×10^{-4}	6.87×10^{-2}	5.01×10^{-1}	1.69×10^{0}
27	100.00	99.82	99.58	99.73	1.26×10^{-3}	1.75×10^{-1}	4.15×10^{-1}	2.75×10^{-1}
28	100.00	99.93	99.13	98.35	1.19×10^{-3}	7.50×10^{-2}	8.66×10^{-1}	1.65×10^{0}
29	100.00	99.66	99.81	99.61	1.48×10^{-5}	3.37×10^{-1}	1.89×10^{-1}	3.94×10^{-1}
80	100.00	99.67	99.59	99.28	1.68×10^{-3}	3.32×10^{-1}	4.13×10^{-1}	7.22×10^{-1}
81	100.00	99.95	99.40	98.71	2.34×10^{-4}	5.25×10^{-2}	5.98×10^{-1}	1.29×10^{0}
82	100.00	99.89	99.12	99.36	1.15×10^{-4}	1.11×10^{-1}	8.82×10^{-1}	6.39×10^{-1}
83	100.00	99.65	99.36	99.19	2.56×10^{-3}	3.47×10^{-1}	6.35×10^{-1}	8.15×10^{-1}
84	100.00	99.82	99.57	99.27	8.66×10^{-4}	1.78×10^{-1}	4.30×10^{-1}	7.33×10^{-1}
85	100.00	99.87	99.55	99.65	1.50×10^{-3}	1.31×10^{-1}	4.54×10^{-1}	1.35×10^{0}
86	100.00	99.81	99.84	99.84	6.47×10^{-4}	1.91×10^{-1}	1.56×10^{-1}	1.61×10^{-1}
87	100.00	99.90	99.02	98.16	3.69×10^{-4}	1.04×10^{-1}	9.76×10^{-1}	1.84×10^{0}
Average				3.81×10^{-4}	8.36×10^{-4}	1.86×10^{-1}	5.62×10^{-1}	9.52×10^{-1}

Table 11 Damage severity in elements estimated by IGA for Scenario 3

No. element	Damage severity				ΔDS (%)			
	Noise level				Noise level			
	0%	1%	3%	5%	0%	1%	3%	5%
24	100.00	97.23	94.88	94.28	3.81×10^{-4}	2.77×10^{0}	5.12×10^{0}	5.72×10^{0}
Average					3.81×10^{-4}	2.77×10^{0}	5.12×10^{0}	5.72×10^{0}

Table 12 Damage severity in elements estimated by IGA for Scenario 4

No. element	Damage severity				ΔDS (%)			
	Noise level				Noise level			
	0%	1%	3%	5%	0%	1%	3%	5%
24	100.00	98.05	95.26	93.80	3.06×10^{-5}	1.95×10^{0}	4.74×10^{0}	6.20×10^{0}
81	99.99	97.92	94.71	94.07	1.23×10^{-2}	2.08×10^{0}	5.29×10^{0}	5.93×10^{0}
Average					6.17×10^{-3}	2.02×10^{0}	5.02×10^{0}	6.07×10^{0}

Table 13 Damage severity in elements estimated by IGA for Scenario 5

No. element	Damage severity				ΔDS (%)			
	Noise level				Noise level			
	0%	1%	3%	5%	0%	1%	3%	5%
24	33.33	30.35	27.62	24.00	3.36×10^{-3}	2.97×10^{0}	5.72×10^{0}	9.33×10^{0}
Average					3.36×10^{-3}	2.97×10^{0}	5.72×10^{0}	9.33×10^{0}

accurately estimating the severity of damage. By applying noise to the input data, the performance of this algorithm is still acceptable.

Similar to the steps explained for damage detection in Scenario 1, the process is repeated for scenarios 2-5. The results of damage detection obtained from the fourth step in scenarios 2-5 are provided in Tables 10-13.

According to the results of damage detection shown in Tables 10-13, the values of ΔDS in the noise level of 0% are very small and close to zero. For other noise levels, the performance of the proposed algorithm is in the acceptable range.

In order to detect damage, the sixth damage scenario is the most crucial challenge in the performance of the suggested algorithm. This scenario is the same as scenario 4, but the end of one of the beams on the first floor only transmits forces and cannot sustain any bending moments. Hence, according to this scenario, there are two different damages in structure. The results of fitness function convergence in Scenario 6 during consecutive generations for different groups are presented in Fig. 9. As shown in Fig. 9, by examining the brace, column, and beam groups, finally, 53 elements enter the fourth step as the elements suspicious to damage. Since the results of brace, column, and beam groups are converged to a value other than zero, it is possible that damaged elements are placed in different groups. Besides, the damage type may be different from the change in elasticity modulus of elements, and damage has not occurred in the element length. Examining the elements suspicious to damage in brace, column, and beam groups in the fourth step, it is observed that the fitness function is considerably reduced but does not converge to zero. This considerable reduction in the fourth step is due to the detection of healthy elements and reducing the number of elements suspicious to damage. Therefore, in this damage scenario, other possible damages in the structure should be checked to make the fitness function ultimately converge to zero. According to Fig. 9(d), eight damaged elements finally remain. Damage detection results from the fourth step are provided in Table 14.

The location of elements suspicious to damage remained from the fourth step with yellow elements is indicated in Fig. 10. In this step, the damage possibility in connection of the beam and column elements suspicious to damage is also examined. For this reason, eight nodes are added for possible damage at the two ends of the beam and column elements suspected to damage, as presented in red in Fig. 10. Therefore, a total of 16 variables are placed in a new search phase. The difference is that the variables related to the damage coefficients of the elements (α_j) have a value between -1 and 0, but the variables related to the connections are defined in such a way that the result is either a value of 0 which represents a rigid connection or a value of 1 which represents a pin connection. It is worth noting that this method can consider continuous values for the connection coefficients (like other elements), which helps the algorithm work effectively even if the connections are semi-rigid. However, since only fully fixed and pin

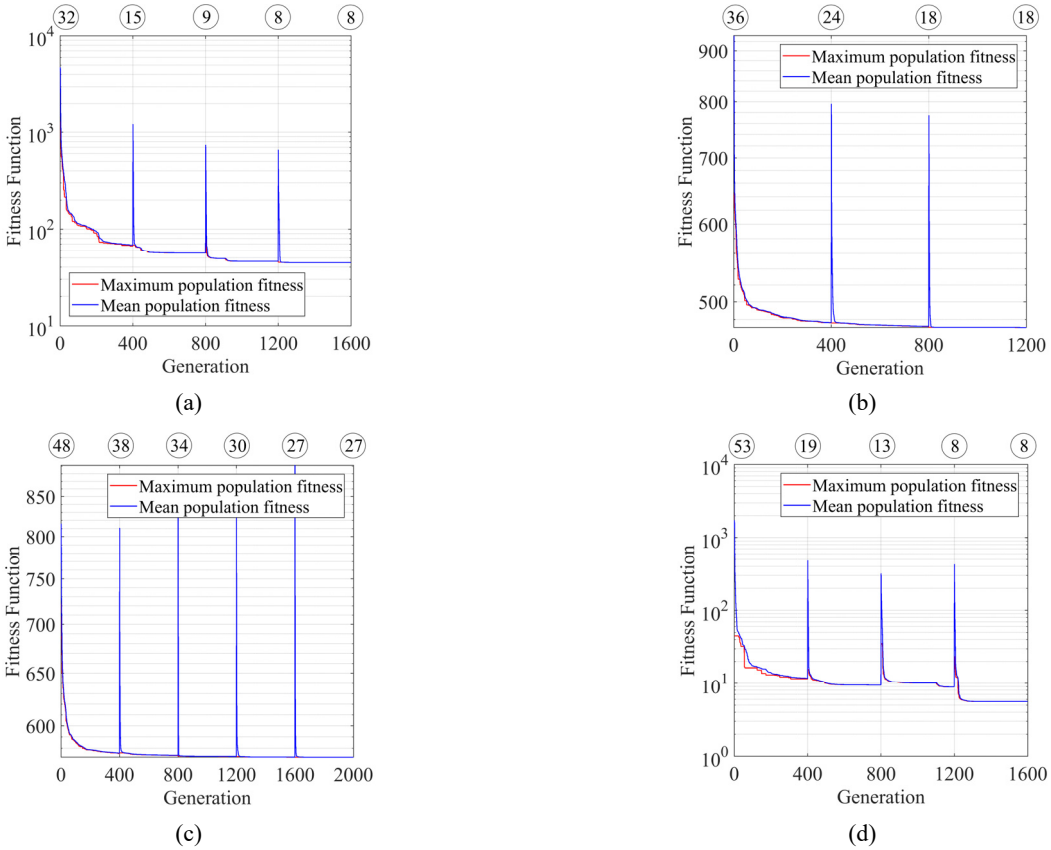

Fig. 9 The convergence process of the Fitness function obtained by IGA for Scenario 6. (a) Braces group; (b) Columns group; (c) Beams group; (d) Suspected damaged elements (0% noise level)

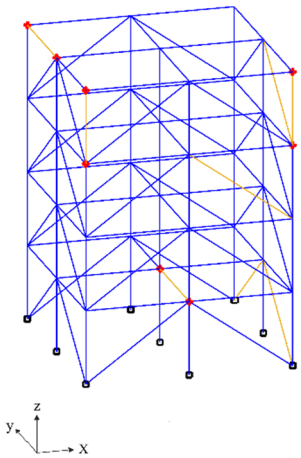

Fig. 10 Remaining elements at the end of fourth step evaluation

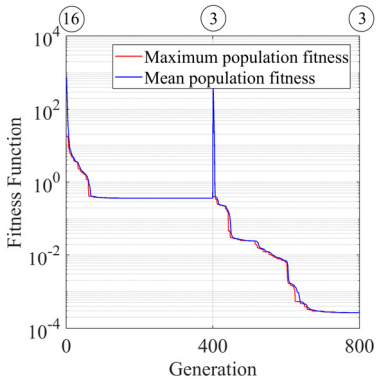

Fig. 11 The convergence process of final step obtained by IGA for Scenario 6 (0% noise level)

connections are considered in the ASCE benchmark structure, two values of 0 and 1 are assigned to the connections.

Results of the new search for elements and connections variables are indicated in Fig. 11. According to this figure, the algorithm finishes after two repetitions, and the fitness function converges to zero. Finally, two braces in the first and third floors, and a connection related to the end of the first floor beam, are detected as damaged elements and connections. The damage severity and ΔDS are presented in Table 15. As is clear from the results, ΔDS is zero for all noise levels. The reason is that the damage to the connection is 0 or 1, i.e., either the connection is healthy (rigid connection) or damaged (pin connection).

5. Experimental study

To investigate the performance of the IGA method in detecting connection damage, a steel belt was utilized as a beam welded continuously and one-sided on an angle profile with a specific thickness. Figs. 12 and 13 show the schematic form of the model, including the beam and seat-angle dimensions, and the test model made in the structural laboratory, respectively.

Table 14 Damage severity in elements estimated by IGA for Scenario 6 (1st detection)

No. element	Damage severity				ΔDS (%)			
	Noise level				Noise level			
	0%	1%	3%	5%	0%	1%	3%	5%
18	88.18	85.23	79.57	69.51	$8.82 \times 10^{+1}$	$8.52 \times 10^{+1}$	$7.96 \times 10^{+1}$	$6.95 \times 10^{+1}$
24	98.44	90.38	82.63	84.41	1.56×10^{0}	9.62×10^{0}	$1.74 \times 10^{+1}$	$1.56 \times 10^{+1}$
25	1.56	11.60	16.37	16.16	1.56×10^{0}	$1.16 \times 10^{+1}$	$1.64 \times 10^{+1}$	$1.62 \times 10^{+1}$
81	100.00	97.38	93.55	90.62	7.47×10^{-6}	2.64×10^{0}	6.45×10^{0}	9.38×10^{0}
88	6.29	37.68	51.42	52.19	6.29×10^{0}	$3.77 \times 10^{+1}$	$5.14 \times 10^{+1}$	$5.22 \times 10^{+1}$
90	3.12	38.26	37.49	37.03	3.12×10^{0}	$3.83 \times 10^{+1}$	$3.75 \times 10^{+1}$	$3.70 \times 10^{+1}$
104	22.08	50.68	55.77	35.52	2.21×10^{0}	$5.07 \times 10^{+1}$	$5.58 \times 10^{+1}$	$3.55 \times 10^{+1}$
111	2.34	17.98	28.75	22.49	2.34×10^{0}	$1.80 \times 10^{+1}$	$2.87 \times 10^{+1}$	$2.25 \times 10^{+1}$
Average					$1.32 \times 10^{+1}$	$3.17 \times 10^{+1}$	$3.67 \times 10^{+1}$	$3.22 \times 10^{+1}$

Table 15 Damage severity in elements estimated by IGA for Scenario 6 (2nd detection)

No. element	Damage severity				ΔDS (%)			
	Noise level				Noise level			
	0%	1%	3%	5%	0%	1%	3%	5%
24	100.00	97.21	95.42	91.18	2.44×10^{-8}	2.79×10^{0}	4.59×10^{0}	8.82×10^{0}
81	100.00	97.74	95.22	91.25	4.79×10^{-5}	2.26×10^{0}	4.78×10^{0}	8.75×10^{0}
Connection	100.00	100.00	100.00	100.00	0.00	0.00	0.00	0.00
Average					1.60×10^{-5}	1.68×10^{0}	3.12×10^{0}	5.86×10^{0}

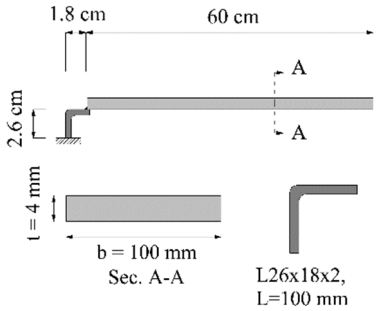

Fig. 12 schematic form of the cantilever beam

Fig. 13 Test model of the beam and seat angle

Since the created cantilever beam has no off-plane motion, it can be regarded as a two-dimensional model. The on-plane horizontal stiffness of the beam is much higher than the vertical and rotational stiffness. Therefore, the horizontal degree of freedom could also be negligible. Therefore, each node of this model is supposed to have one rotational and one vertical translational degree of freedom. The beam equivalent to the actual model is simulated as a 2D beam element with known properties and two spring elements of unknown stiffness, as shown in Fig. 14.

The steel material properties in this model are $E = 2 \times 10^{11}\ N/m^2$ and $\rho = 7850\ kg/m^3$. The total mass of the accessories mounted on the beam for data collection is 224 gr. This can be considered as a uniform dead load for analytical modeling.

The beam is subjected to a vertical point load at a distance of 57.7 cm from the seat angle. The deformation due to this loading condition is shown in Fig. 15.

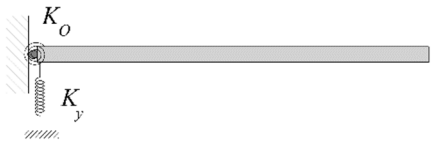

Fig. 14 Modeling of the seat angle using two vertical translational and rotational spring

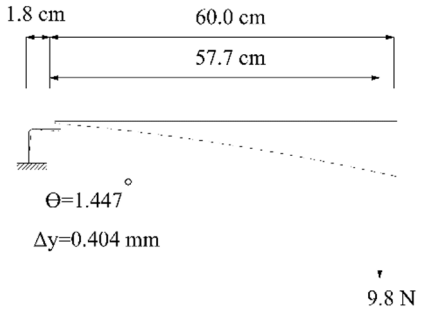

Fig. 15 Deformation of the beam model subjected to static loading

Therefore, the stiffness of this connection is equal to

$$K_\theta = \frac{M}{\theta} = 223.86\ \left(\frac{\text{Nm}}{\text{rad}}\right) \tag{14}$$

$$K_y = \frac{F}{\Delta} = 24245.42\left(\frac{N}{m}\right) \tag{15}$$

Then, the fixity factor of this connection is $\gamma = 29.564\%$ using Eq. (16) (Monforton 1962)

$$\gamma_j = \frac{L}{L + 3EIZ_j} \tag{16}$$

where, L, E, and I are length, elasticity module, and inertia moment of the element, respectively. Z is the inverse of the connection stiffness.

Theoretically, the stiffness of the springs can be in the range of $0 \le K_y \le \infty$. However, from an engineering point of view, a specific upper limit can be assumed in which the frequency does not change considerably. Therefore, the translational stiffness is considered $0 \le K_y \le 2666131\ N/m$ so that the frequency of the structure remains constant up to 3 decimal places. By scaling the translational stiffness to the range of 0 to 1, the rigidity coefficient of the translational spring is

$$SF_1 = \left(\frac{(24245.42 - 0) \times (1 - 0)}{(2666131 - 0)} + 0\right) \times 100 = 0.909\% \tag{17}$$

To determine the fixity factor and rigidity of the springs, the modal strain energy is established as the objective function using the complete first mode. Since only the first mode of the beam is required, 9.8 N static loading applies to the end of the beam, and suddenly eliminated to cause the free vibration. The accelerometer sensors record the acceleration of vertical and rotational DOFs of the beam at the start and end nodes. Then, using the Fourier analysis, the mode shape of the desired DOFs is obtained. To record vertical acceleration, it is just required to install the accelerometer sensor directly on the model so that there is no relative motion between the model and the accelerometer. In the previous research works, translational acceleration was recorded using translational accelerometers. However, in the present study, translational accelerometer sensors, mounted at a certain height of the beam, are used to record rotational acceleration (Fig. 16).

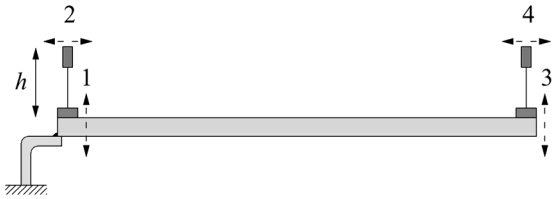

Fig. 16 The location and installation procedure of accelerometer sensors to measure vertical and rotational DOFs

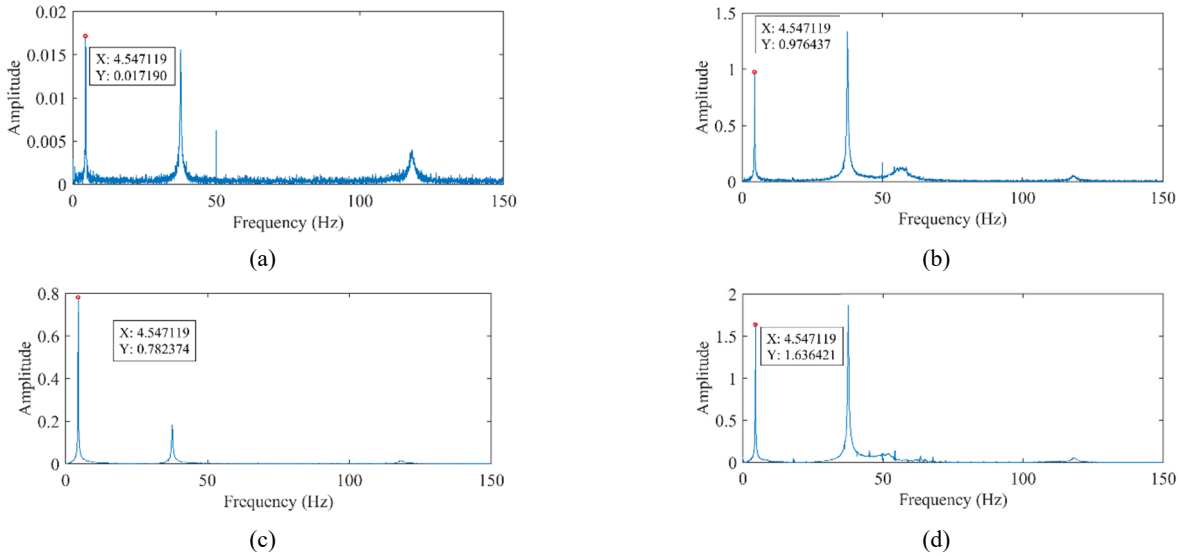

Fig. 17 Fourier analysis of (a) 1st DOF; (b) 2nd DOF; (c) 3rd DOF; (d) 4th DOF

The rotational acceleration is obtained through the following equation

$$\ddot{\theta}_t = \text{Arc}\,Sin\left(\frac{\ddot{x}_t}{h}\right) \simeq \left(\frac{\ddot{x}_t}{h}\right) \tag{18}$$

To minimize rotational acceleration measurement error, the element on which the accelerometer is installed, in addition to its negligible weight, must have high rigidity along its length and at its connection to the beam. Therefore, the plexiglass pieces are used to address this issue. The Fourier analysis of recorded acceleration in 1-4 DOFs is shown in Fig. 17.

By modeling the seat angle as two vertical translational and rotational springs, as shown in Fig. 14, the number of variables is 2. In this case, the MSE of the first mode shape is considered as the objective function. The convergence process of the objective function and the fixity factor of the investigated connection are presented in Figs. 18, and 19. As can be seen, after nearly 40 generations, the search process is stopped, and convergence is achieved.

The convergence process of the fixity factor of the connection estimated by IGA

$$\Delta\gamma = |\gamma_2 - \gamma_1| = 1.208\% \tag{19}$$

$$\Delta SF = |SF_2 - SF_1| = 0.413\% \tag{20}$$

The results revealed that for 2D models, the fixity factor of connections can be determined by obtaining just the first mode shape.

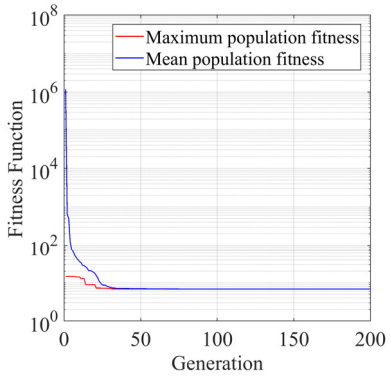

Fig. 18 The convergence process of the objective function obtained by IGA

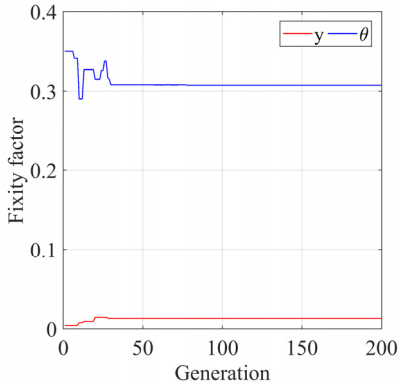

Fig. 19 The convergence process of the fixity factor of the connection estimated by IGA

6. Conclusions

In this paper, an attempt was made to provide practical ideas to improve genetic algorithm and identify the damage based on the least modal information of the structure. Investigations on two numerical models including a 2D truss and a 3D structure showed that in 2D models only one mode, and in 3D models with braces in two perpendicular directions only two perpendicular modes are needed for damage identification. Comparison of IGA algorithm with standard form of GA and DE in 2D truss model showed that the standard algorithms, even with more generations, cannot reach acceptable accuracy using the information of first three modes. According to this method, damage coefficients

of all elements are determined by IGA. In the two-dimensional truss model, due to the small number of elements, all elements formed a single group and entered the damage detection algorithm. After several resuming of the search process and removing healthy elements, the damaged elements were identified with high accuracy. Including the effect of different noise levels revealed that this method has a maximum difference of 2.27% estimating the severity of damage for 0% to 5% noise levels in the DS1 scenario. Considering the large number of variables in 3D ASCE structure, the elements were separately examined in three groups of braces, columns, and beams. Damage coefficients of different groups were introduced to IGA as variables in order to minimize MSE differences of damaged structure and MSE of updated structure. Damage coefficients of different groups were obtained by removing healthy elements and limiting the number of variables. In the next step, the damage coefficients of the suspected damaged elements remaining from the three groups of braces, columns, and beam were estimated by the IGA algorithm**.** If the IGA precisely determines the damage coefficients, the damaged model created from IGA is the main damaged structure, and fitness function will be zero. Results of the study for six different damage scenarios indicated that this method can accurately determine the damage severity in elements by only using two perpendicular modes. As a challenge for performance of the proposed method, different damage scenarios were considered including general and limited damages and different combinations of damage in form of elasticity modulus reduction and damage in connections were considered. The proposed method could achieve the three main targets of detection of damaged elements, determination of the damage type, and estimation of damage severities. Considering 0% to 5% noise levels and the DS5 scenario, the proposed method showed a maximum error of 9.33% in estimating the severity of damage. Comparison of the errors showed that as the number of damaged elements and the severity of the damage increase, the effect of noise on the results decreases.

Then a novel methodology was presented to extract rotational mode shape that contains valuable information about connections. For this purpose, the connection stiffness of a cantilever beam was experimentally studied. In this model, the first mode of the beam at its start and end nodes was used to calculate the objective function. Each node contains a vertical and rotational degree of freedom. The vertical mode shape was obtained by analyzing the vertical acceleration recorded via a sensor mounted on the beam, and the rotational mode shape was obtained by analyzing the horizontal acceleration recorded by the sensor installed at a certain height of the model. The difference between the fixity factor through static methods and the proposed algorithm was 1.208% for rotational spring and 0.413% for translational spring. The results attested to the efficiency of this algorithm to accurately estimate the connection fixity factor.

Acknowledgments

The present study is a part of the first author's PhD thesis at the International Institute of Earthquake Engineering and Seismology, whose support is gratefully appreciated.

References

Alten, K., Ralbovsky, M., Vorwagner, A., Toplitzer, H. and Wittmann, S. (2017), "Evaluation of different monitoring techniques during damage infliction on structures", *Procedia Eng*., **199**, 1840-1845. https://doi.org/10.1016/j.proeng.2017.09.106

Alvandi, A. and Cremona, C. (2006), "Assessment of vibration-based damage identification techniques", *J. Sound Vib*., **292**(1-2), 179-202. https://doi.org/10.1016/j.jsv.2005.07.036

Daei, M., Sokhangou, F. and Hejazi, M. (2017), "A new intelligent algorithm for damage detection in frames via modal properties", *Intell. Build. Int*., **9**(4), 222-236. https://doi.org/10.1080/17508975.2016.1161584

Datta, D. and Dutta, A. (2020), "Structural health monitoring using improved subspace identification method by including rotational degrees of freedom", In: *Advances in Rotor Dynamics*, *Control*, *and Structural Health Monitoring*, Springer, pp. 215-226. https://doi.org/10.1007/978-981-15-5693-7_16

Ding, Z., Li, J. and Hao, H. (2019), "Structural damage identification using improved Jaya algorithm based on sparse regularization and Bayesian inference", *Mech. Syst. Signal Process*., **132**, 211-231. https://doi.org/10.1016/j.ymssp.2019.06.029

Doebling, S.W., Farrar, C.R. and Prime, M.B. (1998), "A summary review of vibration-based damage identification methods", *Shock Vib. Digest*, **30**(2), 91-105.

Ghiasia, R. and Ghasemi, M.R. (2018), "Optimization-based method for structural damage detection with consideration of uncertainties-a comparative study", *Smart Struct. Syst*., *Int. J*., **22**(5), 561-574. https://doi.org/10.12989/sss.2018.22.5.561

Gomes, G.F., Da Cunha, S.S. and Ancelotti, A.C. (2019), "A sunflower optimization (SFO) algorithm applied to damage identification on laminated composite plates", *Eng. Comput*., **35**(2), 619-626. https://doi.org/10.1007/s00366-018-0620-8

Gomes, H. and Silva, N. (2008), "Some comparisons for damage detection on structures using genetic algorithms and modal sensitivity method", *Appl. Mathe. Modell*., **32**(11), 2216-2232. https://doi.org/10.1016/j.apm.2007.07.002

Hester, D., Brownjohn, J., Huseynov, F., Obrien, E., Gonzalez, A. and Casero, M. (2020), "Identifying damage in a bridge by analysing rotation response to a moving load", *Struct. Infrastruct. Eng*., **16**(7), 1050-1065. https://doi.org/10.1080/15732479.2019.1680710

Hormozabad, S.J. and Soto, M.G. (2021), "Real-time damage identification of discrete structures via neural networks subjected to dynamic loading", Health Monitoring of Structural and Biological Systems XV, International Society for Optics and Photonics, 115932O. https://doi.org/10.1117/12.2582482

Huseynov, F., Kim, C., Obrien, E., Brownjohn, J., Hester, D. and Chang, K. (2020), "Bridge damage detection using rotation measurements–Experimental validation", *Mech. Syst. Signal Process*., **135**, 106380. https://doi.org/10.1016/j.ymssp.2019.106380

Johnson, E.A., Lam, H.-F., Katafygiotis, L.S. and Beck, J.L. (2004), "Phase I IASC-ASCE structural health monitoring benchmark problem using simulated data", *J. Eng. Mech*., **130**(1), 3-15.

https://doi.org/10.1061/(ASCE)0733-9399(2004)130:1(3)
Kaveh, A., Hoseini Vaez, S. and Hosseini, P. (2019), "Enhanced vibrating particles system algorithm for damage identification of truss structures", *Scientia Iranica*, **26**(1), 246-256. https://doi.org/10.24200/SCI.2017.4265
Li, J., Wu, B., Zeng, Q. and Lim, C.W. (2010), "A generalized flexibility matrix based approach for structural damage detection", *J. Sound Vib.*, **329**(22), 4583-4587. https://doi.org/10.1016/j.jsv.2010.05.024
Liang, Y., Feng, Q., Li, H. and Jiang, J. (2019), "Damage detection of shear buildings using frequency-change-ratio and model updating algorithm", *Smart Struct. Syst., Int. J.*, **23**(2), 107-122. https://doi.org/10.12989/sss.2019.23.2.107
Meng, F., Yu, J., Alaluf, D., Mokrani, B. and Preumont, A. (2019), "Modal flexibility based damage detection for suspension bridge hangers: A numerical and experimental investigation", *Smart Struct. Syst., Int. J.*, **23**(1), 15-29. https://doi.org/10.12989/sss.2019.23.1.015
Monforton, G.R. (1962), *Matrix analysis of frames with semi-rigid connections*.
Moradipour, P., Chan, T.H. and Gallage, C. (2015), "An improved modal strain energy method for structural damage detection, 2D simulation", *Struct. Eng. Mech., Int. J.*, **54**(1), 105-119. https://doi.org/10.12989/sem.2015.54.1.105
Nobahari, M. and Seyedpoor, S. (2011), "Structural damage detection using an efficient correlation-based index and a modified genetic algorithm", *Mathe. Comput. Modell.*, **53**(9-10), 1798-1809. https://doi.org/10.1016/j.mcm.2010.12.058
Pal, J., Banerjee, S., Chikermane, S. and Banerji, P. (2017), "Estimation of fixity factors of bolted joints in a steel frame structure using a vibration-based health monitoring technique", *Int. J. Steel Struct.*, **17**(2), 593-607. https://doi.org/10.1007/s13296-017-6018-4
Pandey, A. and Biswas, M. (1994), "Damage detection in structures using changes in flexibility", *J. Sound Vib.*, **169**(1), 3-17. https://doi.org/10.1006/jsvi.1994.1002
Pedram, M., Esfandiari, A. and Khedmati, M.R. (2018), "Frequency domain damage detection of plate and shell structures by finite element model updating", *Inverse Problems Sci. Eng.*, **26**(1), 100-132. https://doi.org/10.1080/17415977.2017.1309398
Quaranta, G., Carboni, B. and Lacarbonara, W. (2016), "Damage detection by modal curvatures: numerical issues", *J. Vib. Control*, **22**(7), 1913-1927. https://doi.org/10.1177/1077546314545528
Ramezani, M. and Bahar, O. (2021), "Indirect structure damage identification with the information of the vertical and rotational mode shapes", *Scientia Iranica*. https://doi.org/10.24200/SCI.2021.56842.4939
Ramezani, M., Bathaei, A. and Zahrai, S.M. (2017), "Designing fuzzy systems for optimal parameters of TMDs to reduce seismic response of tall buildings", *Smart Struct. Syst., Int. J.*, **20**(1), 61-74. https://doi.org/10.12989/sss.2017.19.3.269
Seyedpoor, S.M., Norouzi, E. and Ghasemi, S. (2018), "Structural damage detection using a multi-stage improved differential evolution algorithm (Numerical and experimental)", *Smart Struct. Syst., Int. J.*, **21**(2), 235-248. https://doi.org/10.12989/sss.2018.21.2.235
Shahri, A.H. and Ghorbani-Tanha, A. (2017), "Damage detection via closed-form sensitivity matrix of modal kinetic energy change ratio", *J. Sound Vib.*, **401**, 268-281. https://doi.org/10.1016/j.jsv.2017.04.039
Shi, Z., Law, S. and Zhang, L. (1998), "Structural damage localization from modal strain energy change", *J. Sound Vib.*, **218**(5), 825-844. https://doi.org/10.1006/jsvi.1998.1878
Shi, Z., Law, S. and Zhang, L.M. (2000), "Structural damage detection from modal strain energy change", *J. Eng. Mech.*, **126**(12), 1216-1223. https://doi.org/10.1061/(ASCE)0733-9399(2000)126:12(1216)
Silva, M., Santos, A., Figueiredo, E., Santos, R., Sales, C. and Costa, J.C. (2016), "A novel unsupervised approach based on a genetic algorithm for structural damage detection in bridges", *Eng. Applicat. Artif. Intell.*, **52**, 168-180. https://doi.org/10.1016/j.engappai.2016.03.002
Srinivas, V., Ramanjaneyulu, K. and Jeyasehar, C.A. (2011), "Multi-stage approach for structural damage identification using modal strain energy and evolutionary optimization techniques", *Struct. Health Monitor.*, **10**(2), 219-230. https://doi.org/10.1177/1475921710373291
Tiachacht, S., Bouazzouni, A., Khatir, S., Wahab, M.A., Behtani, A. and Capozucca, R. (2018), "Damage assessment in structures using combination of a modified Cornwell indicator and genetic algorithm", *Eng. Struct.*, **177**, 421-430. https://doi.org/10.1016/j.engstruct.2018.09.070
Whalen, T.M. (2008), "The behavior of higher order mode shape derivatives in damaged, beam-like structures", *J. Sound Vib.*, **309**(3-5), 426-464. https://doi.org/10.1016/j.jsv.2007.07.054
Yan, W.-J. and Ren, W.-X. (2014), "Closed-form modal flexibility sensitivity and its application to structural damage detection without modal truncation error", *J. Vib. Control*, **20**(12), 1816-1830. https://doi.org/10.1177/1077546313476724
Yan, W.-J., Huang, T.-L. and Ren, W.-X. (2010), "Damage detection method based on element modal strain energy sensitivity", *Adv. Struct. Eng.*, **13**(6), 1075-1088. https://doi.org/10.1260/1369-4332.13.6.1075
Yang, Q. and Liu, J. (2009), "Damage identification by the eigenparameter decomposition of structural flexibility change", *Int. J. Numer. Methods Eng.*, **78**(4), 444-459. https://doi.org/10.1002/nme.2494
Zheng, T., Luo, W., Hou, R., Lu, Z. and Cui, J. (2020), "A novel experience-based learning algorithm for structural damage identification: simulation and experimental verification", *Eng. Optimiz.*, **52**(10), 1658-1681. https://doi.org/10.1080/0305215X.2019.1668935

CC